

Spring constant of microcantilevers in fundamental and higher eigenmodes

J. Kokavecz¹ and A. Mechler²

¹*Institute for Engineering and Materials Science, University of Szeged, P.O. Box 406, H-6701 Szeged, Hungary*

²*School of Chemistry, Monash University, Clayton, Victoria 3800, Australia*

(Received 15 September 2008; published 4 November 2008)

Microcantilever beams are versatile force sensors used for, among others, microaccelerometry, microelectromechanical systems, and surface force measurements, the most prominent application being atomic force microscopic imaging and force spectroscopy. Bending of the cantilever is used for simple force measurements, while changes in the amplitude or frequency of the fundamental resonance are used to detect small interaction forces or brief perturbations. Spring constants needed for quantitative measurements are determined by “reversing” the force measurements, using either Hooke’s law or the oscillation of the beam. The equality of the Hookian and the oscillating spring constant is generally assumed; however, consistent differences in experimental results suggest otherwise. In this work, we introduce a theoretical formula to describe the relationship between these two spring constants for an Euler-Bernoulli beam. We show that the two spring constants are not equal, although the percentage difference stays in the range of a single digit. We derive a general formula for the determination of effective spring constants of arbitrary eigenmodes of the cantilever beam. We demonstrate that all overtones can be treated with a linear spring - effective mass approach, where the mass remains the same for higher eigenmodes.

DOI: [10.1103/PhysRevB.78.172101](https://doi.org/10.1103/PhysRevB.78.172101)

PACS number(s): 68.37.Ps, 07.79.Lh

I. INTRODUCTION

Accurate measurement of small forces plays a determining role in a wide range of applications from integrated microelectromechanical systems¹ through microaccelerometers (used in, e.g., artificial limbs)^{2,3} to force microscopes.⁴ The required detection limit is shrinking with the size of devices, reaching the range of second-order molecular interactions involved in surface adhesion, conformation changes, antibody-antigen interactions, and protein folding. Characterizing such interactions, in turn, brings into reach the understanding of the rules that govern the molecular world.

The simplest microscopic force sensor is a microcantilever, such as the probe of an atomic force microscope (AFM).⁴ AFM uses a microcantilever equipped with a sharp tip to perform precise measurements of probe-surface interaction force to record an envelope of constant force as the surface morphology. During this process, forces in the order of pN are detected; the AFM is thus an ideal model of microcantilever force sensors. Hence, we approach the problem from the direction of AFM force measurements.

Microcantilevers are frequently described as linear springs. Thus, the linear relationship between the measured (exerted) force and the deflection d of the microcantilever probe can be described by Hooke’s law: $F = k_{st} \times d$ provided that the deflection remains small. The static (Hookian) spring constant (k_{st}) is used for quantitative force-distance measurements⁵ performed through different AFM working modes such as point force spectroscopy, force volume imaging,⁶ pulsed force mode,⁷ and jumping mode.⁸ Another less direct way to determine forces with a microcantilever is by measuring changes in the amplitude or frequency of an oscillating eigenmode,^{9,10} both being influenced by external force fields, arising from, e.g., electric charges, surface energy, or elasticity.^{11–18} To calculate forces or the surface properties that these forces represent, first the spring constant of the cantilever has to be determined.

The importance of the spring constant, however, is not limited to force measurements. The average tip-sample

power dissipation ($\langle P_{ts} \rangle$) during imaging with the oscillating probe, to the first approach, is a linear function of the cantilever spring constant,

$$\langle P_{ts} \rangle = \frac{kA^2\omega_0^2}{2Q} \left(\frac{A_0}{A_{sp}} \sin \phi - 1 \right), \quad (1)$$

where A_0 and A_{sp} are the amplitudes of the probe far from and in intermittent contact with the surface, respectively; Q is the quality factor of the cantilever; ϕ is the phase difference between the drive and probe oscillation; and ω_0 is the angular resonance frequency of the cantilever.^{19,20} The inclusion of nonlinear surface interactions might alter this simple relationship for small oscillating amplitudes, as it was shown in a number of model simulation works;^{12,14,21–24} nevertheless, nondestructive imaging of delicate samples depends on the spring constant. For routine operation, selection of proper probe spring constant and measurement thereof is part of the working protocols. However, when using higher eigenmodes of the cantilever beam, as suggested recently due to presumably higher force sensitivity,^{19,25–29} there is no simple protocol to choose; neither a simple method to measure the effective spring constant of the probe.

To the first approach, from the dimensions and elastic properties of the cantilever beam the Hookian spring constant k_{st} can be calculated. For a rectangular beam, the ratio of the static load and end-point deflection is described by a simple formula,³⁰

$$k_{st} = \frac{a^3bE}{4L^3}. \quad (2)$$

Here, E is the Young modulus, the length of the cantilever is L , while a and b are the cantilever thickness and width, respectively. It was noticed, however, that the effective spring constant often differs from this theoretical one; thus, dynamic measurements are also frequently used for calibration.

Measurement of effective spring constant is frequently done by the added mass, thermal noise, and Sader methods.^{30–33} Of these, the added mass method offers a way to develop a theoretical formula to relate the spring constant measured this way to the Hookian spring constant of the beam. In this method, small masses are attached to the cantilever and the shift of the resonance frequency is measured. The resonance frequency and the added mass are related as

$$\omega_0 = \sqrt{\frac{k_{dy}}{m_{eff} + m_{ad}}} \quad (3)$$

Here, ω_0 , k_{dy} , m_{eff} , and m_{ad} stand for the angular resonance frequency, dynamic spring constant, effective mass of the cantilever, and the added mass, respectively. The dynamic spring constant can be expressed as a function of the $\frac{\partial \omega_0}{\partial m_{ad}}$ derivative using Eq. (3) as follows:

$$k_{dy} = -\frac{\omega_0^3}{2} \frac{1}{\frac{\partial \omega_0}{\partial m_{ad}}}. \quad (4)$$

In practice, k_{dy} and k_{st} are not distinguished and they are approximated to be equal. However, an article by Sidles *et al.*³⁴ suggests without disclosing the details that values of k_{dy} and k_{st} exhibit a 3% difference. In this Brief Report we investigate whether this difference exists. We treat the cantilever as an Euler-Bernoulli beam which was shown to be a good model for small displacements.³⁵ In the second part of this Brief Report, we derive a simple equation which expresses the dynamic spring constant in higher eigenmodes based on the definition given by Eq. (4).

II. MODEL

Euler-Bernoulli beam equation [Eq. (5)] governs the free transverse vibrations $u(x,t)$ of a uniform beam of elastic modulus E , mass density ρ , cross-sectional inertia I , and cross-sectional area A ,

$$EI \frac{\partial^4 u(x,t)}{\partial x^4} + \rho A \frac{\partial^2 u(x,t)}{t^2} = 0. \quad (5)$$

For rectangular beam of width b and height a , the cross-sectional inertia takes a simple form,

$$I = \frac{a^3 b}{12} \quad (6)$$

The general solution of Eq. (5) can be found in many textbooks,^{36,37}

$$u(x,t) = [C_1 \sin(\lambda x) + C_2 \cos(\lambda x) + C_3 \sinh(\lambda x) + C_4 \cosh(\lambda x)] \exp(\omega t). \quad (7)$$

Substituting Eq. (7) into Eq. (5), one can easily derive the dispersion equation that describes the wave number λ as a function of the angular frequency ω ,

$$\lambda = \sqrt[4]{\frac{\rho A}{EI}} \omega. \quad (8)$$

To apply this formula to the added mass method, the boundary conditions are set in the geometry of the experi-

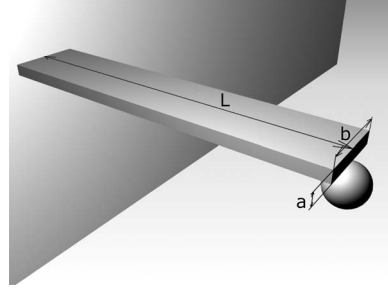


FIG. 1. Model of the microcantilever with added mass. The length of the rectangular microcantilever is L while a and b denote the microcantilever thickness and width.

mental setup. Clamped end is the one fixed to the Z piezo; the added mass is attached to the other end (Fig. 1). Hence, the following boundary conditions apply:

Clamped end ($x=0$),

$$u(0,t) = 0, \quad (9)$$

$$\frac{\partial u(0,t)}{\partial x} = 0. \quad (10)$$

Free end ($x=L$),

$$\frac{\partial^2 u(L,t)}{\partial x^2} = 0, \quad (11)$$

$$EI \frac{\partial^3 u(L,t)}{\partial x^3} = -m_{ad} \frac{\partial^2 u(L,t)}{\partial t^2}. \quad (12)$$

Inserting the general solution into the boundary conditions, we get four equations which are linear in terms of C_i . Consequently, there exist nontrivial solutions for C_i only if the determinant of the coefficient matrix is zero,

$$C_2 + C_4 = 0,$$

$$\lambda C_1 + \lambda C_3 = 0$$

$$-\lambda^2 \sin(\lambda L) C_1 + (-\lambda^2) \cos(\lambda L) C_2 + \lambda^2 \sinh(\lambda L) C_3 + \lambda^2 \cosh(\lambda L) C_4 = 0,$$

$$\left[-\frac{\rho A}{m_{ad}} \cos(\lambda L) + \lambda \sin(\lambda L) \right] C_1 + \left[\frac{\rho A}{m_{ad}} \sin(\lambda L) + \lambda \cos(\lambda L) \right] C_2 + \left[\frac{\rho A}{m_{ad}} \cosh(\lambda L) + \lambda \sinh(\lambda L) \right] C_3 + \left[\frac{\rho A}{m_{ad}} \sinh(\lambda L) + \lambda \cosh(\lambda L) \right] C_4 = 0. \quad (13)$$

By introducing a new variable $\alpha = \lambda L$, the determinant can be written as follows:

$$[1 + \cos(\alpha) \cosh(\alpha)] + \frac{\alpha m_{ad}}{\rho A L} [\cos(\alpha) \sinh(\alpha) - \sin(\alpha) \cosh(\alpha)] = 0. \quad (14)$$

For any given m_{ad} Eq. (14) can be satisfied by an infinite

number of $\alpha_i(m_{\text{ad}})$ where $\alpha_i(m_{\text{ad}})$ corresponds to the i th overtone of the cantilever. The fundamental mode is denoted by $i=0$. The eigenfrequency of the i th overtone while its end is loaded with a mass (m_{ad}) can be expressed as follows:

$$\omega_i(m_{\text{ad}}) = \alpha_i^2(m_{\text{ad}}) \sqrt{\frac{EI}{\rho AL^4}}. \quad (15)$$

To calculate the dynamic spring constant using Eq. (4), we have to calculate the derivatives $\frac{\partial \alpha_i}{\partial m_{\text{ad}}}$ and $\frac{\partial \omega_i}{\partial m_{\text{ad}}}$. This derivative in general depends on m_{ad} . However, if we assume that the added mass is very small, more precisely $m_{\text{ad}} \rightarrow 0$, then we get a simple form for $\frac{\partial \alpha_i}{\partial m_{\text{ad}}}$,

$$\left. \frac{\partial \alpha_i}{\partial m_{\text{ad}}} \right|_{m_{\text{ad}}=0} = -\frac{\alpha_i(0)}{\rho AL}. \quad (16)$$

By substituting Eq. (16) into Eq. (15), we get the form of $\frac{\partial \omega_i}{\partial m_{\text{ad}}}$ as follows:

$$\left. \frac{\partial \omega_i}{\partial m_{\text{ad}}} \right|_{m_{\text{ad}}=0} = \frac{-2\alpha_i^2(0)}{L^3} \sqrt{\frac{EI}{\rho^3 A^3}}. \quad (17)$$

To calculate the dynamic spring constant for the fundamental mode (k_{dy}), we substitute the expression of $\frac{\partial \omega_i}{\partial m_{\text{ad}}}$ [given by Eq. (17)] into Eq. (4) and we get

$$k_{\text{dy}} = \frac{\alpha_0^4(0) EI}{4 L^3}. \quad (18)$$

Here, $\alpha_0^4(0)$ can be evaluated numerically using Eq. (14) resulting in the analytical form of k_{dy} ,

$$k_{\text{dy}} = \frac{1}{3.8828} \frac{a^3 b E}{L^3}. \quad (19)$$

Now, we can quantitatively compare k_{st} [given by Eq. (2)] and k_{dy} [given by Eq. (19)]. First, we can establish that the two spring constants are not equal; the value of k_{dy} is indeed about 3% larger than k_{st} , as suggested by Sidles *et al.*³⁴ Hence, this theoretical analysis shows that cantilever spring constant values acquired from dynamic calibration must be corrected if the cantilever is used for static force measurement. Second, it is also remarkable that the analysis presented above describes the dynamic spring constant of not only the fundamental frequency but also arbitrary overtones of the cantilever. The dynamic spring constant of the i th overtone of the cantilever can be given as

$$k_{\text{dy}}^i = \frac{\alpha_i^4(0) EI}{4 L^3}. \quad (20)$$

In practice it is more useful to define the spring constants of the overtones as a function of measurable quantities like resonance frequencies. Combining Eqs. (15) and (20), we get the following simple formula:

$$k_{\text{dy}}^i = k_{\text{dy}}^0 \frac{\omega_i^2}{\omega_0^2}. \quad (21)$$

That is, for a rectangular cantilever, the ratio of spring constants of any overtones and the fundamental mode equals the

TABLE I. Relative eigenfrequencies and spring constants of the first three overtones of a rectangular microcantilever.

| Mode number | Relative frequency | Relative spring constant |
|-------------|--------------------|--------------------------|
| 0 | 1.0000 | 1.0000 |
| 1 | 6.2669 | 39.2739 |
| 2 | 17.5475 | 307.9141 |
| 3 | 34.3861 | 1182.4012 |

square of the ratio of the corresponding eigenfrequencies. Relative spring constants and resonance frequencies of the first three overtones are listed in Table I.

One can notice that the spring constant rapidly increases with the mode number as also suggested by Sidles *et al.*³⁴ This result is especially important when considering AFM operation at higher eigenmodes. Presuming the validity of Eq. (1), imaging force will increase substantially, thus the advantage gained with the wider bandwidth of the overtones^{23,38} might be lost this way. It remains unclear, however, which effect will dominate. Further modeling work is underway to evaluate this issue.

An important consequence of Eq. (21) is that the $k_{\text{dy}}^i / \omega_i^2$ ratio is constant for all i . This means that if the overtones of the cantilever are modeled as simple spring-mass systems, the effective mass values are the same for all overtones. Thus, in this respect, different overtones behave like linear springs of the same masses and different spring constants. Notably, previous works based on modal analysis suggested the change of effective mass,^{39,40} however, with different boundary conditions. These works included a ‘‘concentrated’’ tip-surface interaction term that induce a multimodal cantilever response.

Equation (4) can be also used to describe the dependence of the dynamic spring constants on the added mass. We calculated the dynamic spring constant as a function of added mass for the fundamental mode and the first two overtones

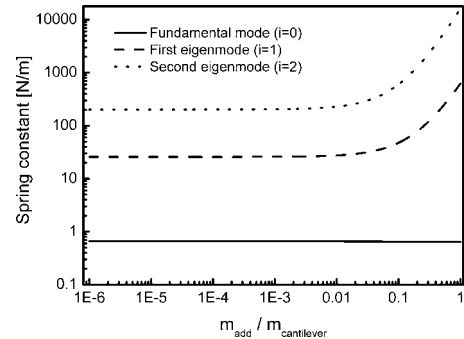


FIG. 2. Dynamic spring constants of the fundamental (solid line), first (dashed line), and second overtones (dotted line) vs added mass ratio. Cantilever data match with the commercial MikroMasch NSC36 C cantilever ($a=1 \mu\text{m}$, $b=35 \mu\text{m}$, $L=130 \mu\text{m}$, nominal spring constant 0.6 N/m , and nominal resonance frequency 75 kHz). It can be seen that while the fundamental mode remains remarkably constant when the added mass changes 10^{-6} – 1 times from the cantilever mass, the harmonic modes become significantly harder with the increasing added mass.

by solving Eq. (4) numerically. Geometry of a commercial soft tapping mode cantilever (MikroMasch NSC36 C) was used. Results are depicted in Fig. 2. Interestingly, the fundamental mode shows a different behavior compared to the overtones; while it remains nearly constant within the range of 10^{-6} to 1 (added mass over cantilever mass), the spring constants of overtones significantly increase toward larger added masses. This increase suggests that the linear spring model is suitable for the fundamental mode, while only applicable to small masses for the higher eigenmodes.

In summary, we deduced a formula that relates the dynamic (resonant) and the Hookian (bending) spring constants of an Euler-Bernoulli microcantilever beam. We found that the dynamic spring constant is $\sim 3\%$ higher than the Hookian spring constant. We presented a general formula to determine effective spring constants of arbitrary overtones of the cantilever beam and thus accurately calculate interaction forces

when using overtones for AFM imaging or force sensing. We described the effect of added mass on the spring constant, which is unchanging for the fundamental mode, but is non-linear for the higher eigenmodes. As higher overtones of the cantilever beam are considered for fast AFM operation, our results provide the means of calculating working characteristics of such systems.

ACKNOWLEDGMENTS

Financial support from grants of the Hungarian Scientific Research Fund (OTKA) under Grants No. TS049872 and No. TO46394, grants of OMFB of the Hungarian Ministry of Culture and Education under Grant No. 01628/2006, and Australian Research Council under Grants No. DP0662816 and No. DP0663290 are kindly acknowledged. A.M. acknowledges a Monash Fellowship.

- ¹ *Smart Sensors and MEMS*, edited by S. Y. Yurish and M. T. S. R. Gomes (Kluwer Academic, Dordrecht, 2004), Chap. 11.
- ² H. Chen, J. Li, and D. Chen, *J. Adhes. Sci. Technol.* **20**, 307 (2006).
- ³ C. De Angelis, V. Ferrari, D. Marioli, E. Sardini, M. Serpelloni, and A. Taroni, *Sens. Actuators, A* **135**, 197 (2007).
- ⁴ G. Binnig, C. F. Quate, and C. Gerber, *Phys. Rev. Lett.* **56**, 930 (1986).
- ⁵ H. J. Butt, B. Cappella, and M. Kappl, *Surf. Sci. Rep.* **59**, 1 (2005).
- ⁶ VEECO, Multimode Spm Instruction Manual, 1999.
- ⁷ H. U. Krottil, T. Stifter, H. Waschipyk, K. Weishaupt, S. Hild, and O. Marti, *Surf. Interface Anal.* **27**, 336 (1999).
- ⁸ F. Moreno-Herrero, J. Colchero, J. Gomez-Herrero, and A. M. Baro, *Phys. Rev. E* **69**, 031915 (2004).
- ⁹ B. Anczykowski, D. Kruger, and H. Fuchs, *Phys. Rev. B* **53**, 15485 (1996).
- ¹⁰ N. Burnham, S. P. Baker, and H. M. Pollock, *J. Mater. Res.* **15**, 2006 (2000).
- ¹¹ D. M. Czajkowsky, M. J. Allen, V. Elings, and Z. Shao, *Ultramicroscopy* **74**, 1 (1998).
- ¹² N. Burnham, O. P. Behrend, F. Oulevey, G. Gremaud, P.-J. Gallo, D. Gourdon, E. Dupas, A. J. Kulik, H. M. Pollock, and G. A. D. Briggs, *Nanotechnology* **8**, 67 (1997).
- ¹³ R. Garcia and A. San Paulo, *Phys. Rev. B* **60**, 4961 (1999).
- ¹⁴ A. Mechler, J. Kokavecz, P. Heszler, and R. Lal, *Appl. Phys. Lett.* **82**, 3740 (2003).
- ¹⁵ A. Mechler, J. Kopniczky, J. Kokavecz, A. Hoel, C. G. Granqvist, and P. Heszler, *Phys. Rev. B* **72**, 125407 (2005).
- ¹⁶ C. Loppacher, M. Guggisberg, O. Pfeiffer, E. Meyer, M. Bamberlin, R. Luthi, R. Schlittler, J. K. Gimzewski, H. Tang, and C. Joachim, *Phys. Rev. Lett.* **90**, 066107 (2003).
- ¹⁷ M. Gauthier, R. Perez, T. Arai, M. Tomitori, and M. Tsukada, *Phys. Rev. Lett.* **89**, 146104 (2002).
- ¹⁸ H. Hölscher, W. Allers, U. D. Schwarz, A. Schwarz, and R. Wiesendanger, *Phys. Rev. Lett.* **83**, 4780 (1999).
- ¹⁹ A. San Paulo and R. Garcia, *Phys. Rev. B* **66**, 041406(R) (2002).
- ²⁰ J. P. Cleveland, B. Anczykowski, A. E. Schmid, and V. B. Elings, *Appl. Phys. Lett.* **72**, 2613 (1998).
- ²¹ O. P. Behrend, F. Oulevey, D. Gourdon, E. Dupas, A. J. Kulik, G. Gremaud, and N. A. Burnham, *Appl. Phys. A: Mater. Sci. Process.* **66**, S219 (1998).
- ²² J. Kokavecz, Z. L. Horváth, and A. Mechler, *Appl. Phys. Lett.* **85**, 3232 (2004).
- ²³ J. Kokavecz, O. Marti, P. Heszler, and A. Mechler, *Phys. Rev. B* **73**, 155403 (2006).
- ²⁴ G. Bar, R. Brandsch, M. Bruch, L. Delineau, and M. H. Whangbo, *Surf. Sci.* **444**, L11 (2000).
- ²⁵ N. F. Martinez, S. Patil, J. R. Lozano, and R. Garcia, *Appl. Phys. Lett.* **89**, 153115 (2006).
- ²⁶ R. Proksch, *Appl. Phys. Lett.* **89**, 113121 (2006).
- ²⁷ R. W. Stark, N. Naujoks, and A. Stemmer, *Nanotechnology* **18**, 065502 (2007).
- ²⁸ O. Sahin, C. F. Quate, O. Solgaard, and A. Atalar, *Phys. Rev. B* **69**, 165416 (2004).
- ²⁹ J. R. Lozano and R. Garcia, *Phys. Rev. Lett.* **100**, 076102 (2008).
- ³⁰ J. P. Cleveland, S. Manne, D. Bocek, and P. K. Hansma, *Rev. Sci. Instrum.* **64**, 403 (1993).
- ³¹ N. A. Burnham, X. Chen, C. S. Hodges, G. A. Matei, E. J. Thoreson, C. J. Roberts, M. C. Davies, and S. J. B. Tandler, *Nanotechnology* **14**, 1 (2003).
- ³² D. A. Mendels, M. Lowe, A. Cuenat, M. G. Cain, E. Vallejo, D. Ellis, and F. Mendels, *J. Micromech. Microeng.* **16**, 1720 (2006).
- ³³ John E. Sader, Ian Larson, Paul Mulvaney, and Lee R. White, *Rev. Sci. Instrum.* **66**, 3789 (1995).
- ³⁴ J. A. Sidles, J. L. Garbini, K. J. Bruland, D. Rugar, O. Züger, S. Hoen, and C. S. Yannoni, *Rev. Mod. Phys.* **67**, 249 (1995).
- ³⁵ R. W. Stark and W. M. Heckl, *Rev. Sci. Instrum.* **74**, 5111 (2003).
- ³⁶ *Shock and Vibration Handbook*, edited by C. M. Harris and A. G. Piersol (McGraw-Hill, New York, 2002), Chap. 7.
- ³⁷ S. G. Kelly, *Schaum's Outline of Mechanical Vibrations* (McGraw-Hill, New York, 1996).
- ³⁸ J. Mertz, O. Marti, and J. Mlynek, *Appl. Phys. Lett.* **62**, 2344 (1993).
- ³⁹ R. W. Stark, G. Schitter, M. Stark, R. Guckenberger, and A. Stemmer, *Phys. Rev. B* **69**, 085412 (2004).
- ⁴⁰ W. L. Wang and S. J. Hu, *Appl. Phys. Lett.* **87**, 183506 (2005).